

Aggregation in a Protein–Surfactant System. The Interplay between Hydrophobic and Electrostatic Interactions

Anna Stenstam,* Daniel Topgaard, and Håkan Wennerström

Physical Chemistry 1, Lund University, P. O. Box 124, S-221 00 Lund, Sweden

Received: November 12, 2002; In Final Form: January 28, 2003

By precipitating a complex salt Ly(OS)_8 of the positively charged protein lysozyme and the anionic surfactant octyl sulfate OS^- , one can generate a true ternary system: water– Ly(OS)_8 –NaOS. Using NMR diffusometry and UV spectroscopy measurements the thermodynamic parameters of the association processes have been determined. The solubility product of the complex salt, K_s , is 10^{-28} M^9 .¹ On addition of excess surfactant the complex salt is solubilized into micelles that form at a critical association concentration of 74 mM which is nearly a factor of 2 lower than the CMC of 133 mM. At higher protein and surfactant concentrations these micelles first coexist with gel aggregates. The thermodynamically stable gel phase is observed at protein concentrations higher than 7 wt % and has a stoichiometry of around 28 OS^- per protein molecule. Thereafter, in the presence of more than ca. 30 OS^- per protein, micelles containing a single lysozyme molecule are formed from the gel aggregates. This rich aggregation pattern can be described as caused by a combination of an attractive hydrophobic interaction between hydrophobic patches on the protein surface and the surfactant hydrocarbon chain, and a composition-dependent electrostatic interaction between charged amino acids and the surfactant headgroup. The net force is attractive up to a ratio of surfactant to protein of 8, after which it becomes increasingly repulsive. The gel phase occurs as a compromise between the attractive hydrophobic interaction and the relatively weak electrostatic repulsion.

Introduction

In an oppositely charged protein–surfactant system the colloidal forces that control the stability of the solution are all manifested. Both inter- and intra- hydrophobic attraction competes with a composition-dependent electrostatic interaction. Knowledge of such a system in terms of the fundamental forces makes it possible to extend to a more general idea of colloidal association and stability. It is therefore also a step closer to understanding protein self-aggregation, which possibly is the reason behind several biological malfunctions such as Alzheimer's disease.²

The binding of ionic surfactant molecules to oppositely charged proteins has been studied extensively by dominantly light scattering, fluorescence probe, and calorimetric methods. The questions of interest have often been to define the saturation level of surfactants per protein molecule and to understand the structure of the saturated complexes.^{3–6} The concentrations have been such that the phase transitions with increasing surfactant-to-protein ratio can be expressed as an initial precipitation of a stoichiometric complex salt, followed by a resolubilization to a charged complex.⁷ It is the latter soluble complex that has received major attention in the past. The present work, with lysozyme and sodium octyl sulfate, SOS, features a different resolubilization route, via a gel phase. The phenomenon of gel formation was in this context first reported by Morén and Khan as a general behavior of lysozyme–alkyl sulfate–water systems.⁸

Thus, the three aggregates observed in the lysozyme–sodium octyl sulfate–water systems can be expressed as a stoichiometric precipitate, a gel, and a charged soluble protein–surfactant complex. In a recent report on the analogue lysozyme–sodium dodecyl sulfate we concluded that the observed aggregates were equilibrium structures and discussed the phase behavior in terms of a thermodynamic model.¹

In this paper we focus on properties of the solution phase even prior to the resolubilization of the precipitated complex salt. The resolubilization is proposed to be preconditioned by self-aggregation of the surfactant molecules, and selecting a surfactant with a high CMC provides better opportunities to study the onset of the solubilization.⁸ Using NMR diffusometry it has been possible to follow the surfactant and protein diffusion.

NMR diffusometry has proven to be a most useful technique in the study of self-aggregating systems.⁹ The method monitors molecular displacements over micrometer-distances, which makes it sensitive to aggregate structures. Hence, the obtained self-diffusion coefficients D may be interpreted in terms of solution microstructure.

Here, the method of NMR is used both to answer the question if the resolubilization is due to surfactant micellization and to examine the diffusion characteristics of the soluble charged complex. As mobilities are related to structure, new data can be added to the discussion on the structure of the complex. The approach to measure protein and surfactant diffusion to study interactions was first presented by Chen et al. in a study of bovine serum albumin and SDS.¹⁰ In the present study the diffusion data prove to be of great value in understanding the

* Author to whom correspondence should be sent. Fax: +46-46-222-4413. E-mail: anna.stenstam@fekem1.lu.se.

phase behavior in molecular terms and have given further insight into the process of resolubilization.

The possibility of connecting the observed phase behavior with an understanding of the underlying force balance is greatly facilitated through the use of the true ternary system. The experimentally defined location of the three-phase triangle ($S + G + L$) is here analyzed in terms of the chemical potential of sodium octyl sulfate. This approach gives further support to the idea that the aggregates are thermodynamically stable phases. The partitioning of the free energies into electrostatic and hydrophobic contributions has been achieved by solving the Poisson–Boltzmann equation.¹¹

Experimental Section

(a) Materials. Lysozyme L-6876 from chicken egg white, three times crystallized and dialyzed, was obtained from Sigma. Sodium octyl sulfate, SOS, was obtained from Merck, and D_2O (>99.8%) from Dr. Glaser. All chemicals were used as received.

The complex salt lysozyme–octyl sulfate, $Ly(OS)_8$, was prepared by precipitating the protein–surfactant complex from an aqueous solution. The isoelectric point of lysozyme is at pH 11 and without any buffers present the pH of the solution is 6.5; which renders the protein lysozyme a positive net charge of eight.¹² Consequently the stoichiometric equilibrium of charges, i.e., the molar ratio of SOS to lysozyme for the solid complex, is eight.¹³ The precipitated complex salt was rinsed with Millipore filtered water from sodium, chlorine, and acetate ions and finally freeze-dried. This protocol has proven to be successful for the analogue salt lysozyme–dodecyl sulfate.¹

(b) Phase Diagram Determination. All samples were prepared in screw-capped vials. Close to the different phase limits, 40 compositions were studied within the concentration regime 80–100 wt % water. The nature of the samples was determined by visual inspection after two weeks and then checked for possible time evolution over several months. The two-phase dispersion of gel in isotropic solution was signaled by a bluish color, and by the presence of a wide, solidlike signal in the 1H NMR spectrum.

(c) NMR Diffusometry. NMR experiments were performed at a temperature of 298 K on a Bruker DMX 200 spectrometer operating at a proton resonance frequency of 200.13 MHz. Magnetic field gradients were generated in a Bruker DIFF-25 gradient probe driven by a Bruker BAFPA-40 unit. The self-diffusion of lysozyme and SOS was followed with the pulsed-field gradient-stimulated echo (PFG STE) NMR technique.¹⁴ This method consists of a stimulated echo, $90^\circ - \tau_1 - 90^\circ - \tau_2 - 90^\circ - \tau_1 - \text{echo}$, with one magnetic field gradient pulse with length δ and strength G in each τ_1 period. $\Delta = \tau_1 + \tau_2$ is the time between the leading edges of the gradient pulses. In the experiments presented here we used $\delta = 1$ ms, $\Delta = 22$ ms, and G was increased linearly to a maximum value of 9.5 T/m in 20 steps. Between each scan, a recycle delay of 1 s was allowed for relaxation. This time is not sufficient for complete relaxation of all species. However, control experiments performed with a recycle delay of 5 s yielded identical results. The total experiment time could thus be greatly reduced by using a short recycle delay.

The echo intensity I is given by

$$I = I_0 e^{-(\gamma G \delta)^2 (\Delta - \delta/3) D} \quad (1)$$

where I_0 is the intensity in the absence of gradients and γ is the gyromagnetic ratio.¹⁵ The experimental parameters are combined

into the variable $k = (\gamma G \delta)^2 (\Delta - \delta/3)$. Equation 1 is valid for the signal intensity in each channel of the spectrum obtained by the Fourier transform of the second half of the echo originating from a single freely diffusing species.^{16,17} In the present system there is an overlap of methylene peaks from SOS and lysozyme. In this case the signal is given by

$$I/I_0 = f e^{-k D_{SOS}} + (1 - f) e^{-k D_{Lys}} \quad (2)$$

where f is the fraction of the signal contributed to by SOS. The diffusion coefficient of lysozyme, D_{Lys} was determined with a fit of eq 1 to the area of the signal originating from the aromatic hydrogens at 7–8 ppm. This value was used as a frozen parameter in the evaluation of D_{SOS} and f from a fit of eq 2 to the area of methylene peak at 1 ppm.

NMR self-diffusion measurements were performed on three different sets of samples. The concentration of protein was at all times 2.2 mM while the surfactant concentration was varied between 13 and 1300 mM, which is below the limit where a hexagonal structure is favored.¹⁸ First the supernatants in equilibrium with precipitated complex salt were studied. Here, the samples were left to equilibrate in screw-capped vials for at least one week before being centrifuged at 3750 rpm. Thereafter, 400 μ L of the supernatant was transferred to 5-mm NMR-tubes. Second, completely solubilized samples were analyzed. After an equally long equilibration time, 400 μ L was transferred to 5 mm NMR-tubes. The third set of experiments was performed on the bluish solutions. When the bluish solution was in equilibrium with precipitate, the supernatant was transferred after centrifugation. The bluish solutions were in all reported NMR measurements homogeneous dispersions. Although these dispersions consist of both micellar solution and gel particles, the signal from the diffusing protein and surfactant arise only from the micellar complex due to slow exchange and the fast relaxation in the gel. This was confirmed by a set of samples where the micellar phase was separated from the gel by centrifugation at 3750 rpm for 48 h.

(d) Ultraviolet Spectroscopy. To quantitatively follow the resolubilization of the solid $Ly(OS)_8$ with increasing concentration of SOS, the concentration of lysozyme in the supernatant was measured as described previously.¹

Results and Discussion

1. Phase Behavior of the Ternary System $Ly(OS)_8$ –SOS–Water. The system $Ly(OS)_8$ –SOS–water displays three different aggregates, solid (S), gel (G), and soluble complex (L_1) and the corresponding two- and three-phase equilibria. The phase behavior of three-component systems is commonly described by ternary phase diagrams. An alternative way to display the phase transitions and equilibria is given in Figure 1, which is based on a combination of information from visual observation of samples as well as UV and NMR measurements. The evolution of the three aggregates that contain lysozyme is shown as a function of increasing SOS concentration and it is possible to get a combined picture of the parallel developments through the different areas. The fraction of protein in each phase applies for a constant 3 wt % lysozyme. It is this series that has been analyzed by UV and NMR.

On adding SOS, the complex salt $Ly(OS)_8$ is first precipitated as a result of the electrostatic and hydrophobic attraction between octyl sulfate and lysozyme. The concentration of lysozyme monomers in equilibrium with the precipitate is according to the solubility product very low. When a critical concentration of sodium octyl sulfate is reached, lysozyme

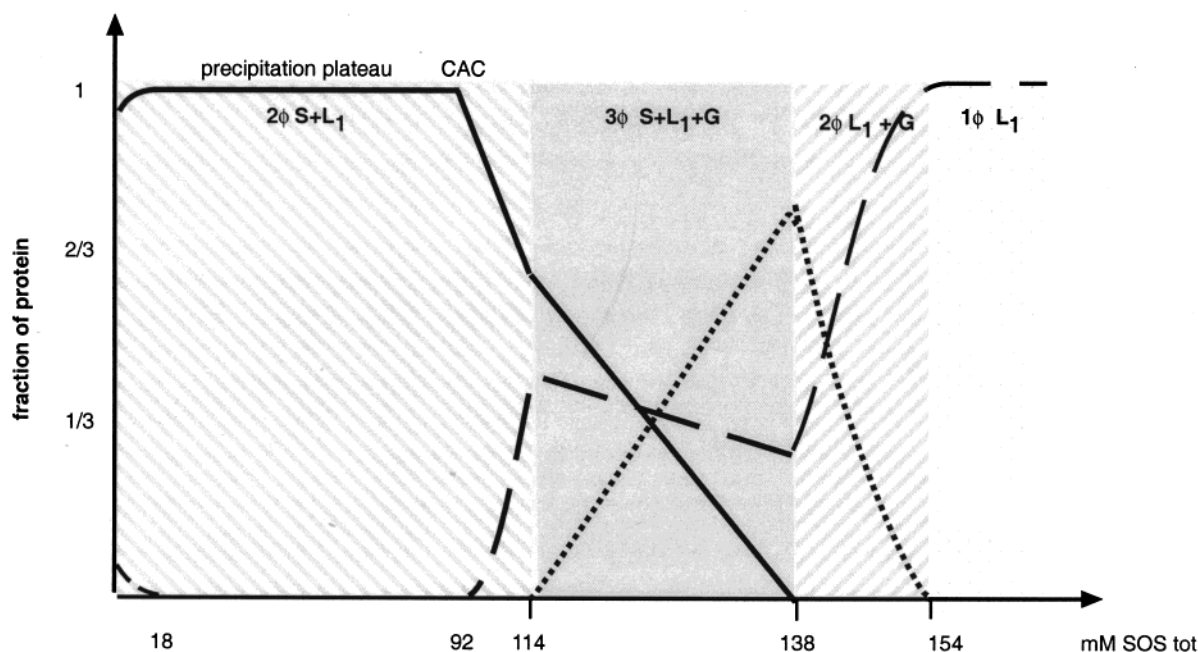


Figure 1. The fraction of lysozyme in the different phases as a function of increasing SOS concentration; full line, the solid $\text{Ly}(\text{OS})_8$; dashed line, lysozyme as monomers or micelles in L_1 ; dotted line, the gel. The amount of protein is held constant at a concentration of 3.0 wt % (2.2 mM) lysozyme and the different shades denote different areas of the phase diagram.

begins to be resolubilized from the solid complex. UV-absorbance measurements reveal that below a total surfactant concentration of 92 mM no detectable amount of lysozyme is present in the supernatants in equilibrium with the solid complex. However, at this point almost all of the stoichiometric amount of surfactant, 8×2.2 mM, is still precipitated with the protein and consequently the free SOS concentration is only 74 mM. We refer to this as the critical association concentration, CAC, since NMR diffusometry shows that the surfactant molecules display monomeric behavior up to this point. The reduction by approximately 50% relative to the CMC of 133 mM is consistent with the general behavior of ionic surfactants in solution with other oppositely charged amphiphilic or hydrophobic compounds.¹⁹ The aggregate formed at CAC is a protein–surfactant micelle. Thus, before CAC the L_1 phase in equilibrium with solid $\text{Ly}(\text{OS})_8$ is a surfactant monomer solution, while after CAC it is a solution of mixed micelles and surfactant monomers.

At concentrations slightly higher than CAC (114 mM), a third associative structure, the gel, appears. The compositions represent the three-phase equilibria of the conventional three-phase triangle. As a guide for the discussion of this paper the compositions of the corners that define the three-phase triangle are given in Table 1.

TABLE 1: Compositions of the Corners That Define the Three-Phase Triangle

corner	L_1	G	S
wt % $\text{Ly}(\text{OS})_8$	1.2	7.0	100
wt % SOS	2.0	3.3	0

Within the three-phase triangle the phase rule is such that the compositions of the different phases are constant while the respective amount change. The solid is further resolubilized and lysozyme enters both gel aggregates and micelles. In the series presented here the amount of gel increases while the L_1 phase is decreasing. This is an effect of the orientation of the three-phase triangle in respect to the triangular phase diagram.

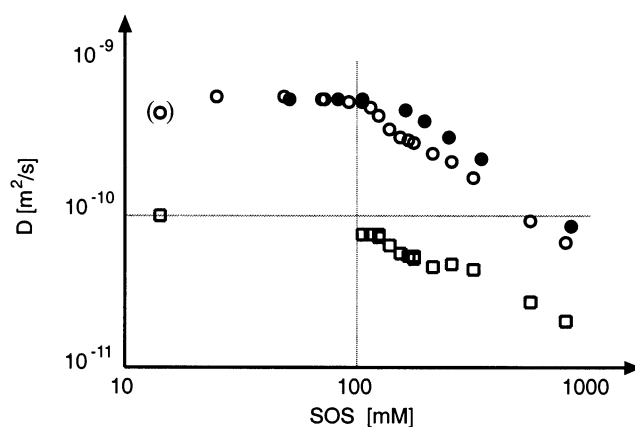


Figure 2. Measured diffusion coefficients; filled circles, SOS in the binary system $\text{SOS}-\text{D}_2\text{O}$; empty circles, SOS in the ternary system; squares, lysozyme in the ternary system. The concentration of protein was 2.2 mM in all samples. The measured SOS diffusion within parentheses is uncertain due to the very low concentration in the supernatant.

When no solid remains, the samples are two-phase equilibria between gel and L_1 . These appear as homogeneous bluish solutions of fairly low viscosity. The dispersions do not settle spontaneously but separate in a bluish gel phase and an L_1 supernatant on centrifugation.

At higher SOS concentrations, a single isotropic, fully transparent solution phase of protein–surfactant micelles and SOS monomers is formed. The behavior follows the general trend described by Morén et al. and theoretically analyzed by us in a previous paper on the aggregation of lysozyme and dodecyl sulfate.^{1,8}

2. NMR Diffusometry. Both the surfactant and the protein diffusional characteristics are shown in Figure 2 together with the surfactant diffusion coefficient in the binary system $\text{SOS}-\text{D}_2\text{O}$. The monomer diffusion rate is measured to be $5.5 \times 10^{-10} \text{ m}^2/\text{s}$, consistent with earlier measurements.²⁰ Similarly, in the absence of surfactant the diffusion coefficient of the lysozyme

molecules is consistent with the fact that it is predominantly in monomeric form in the concentration,²¹ salt, and pH interval²² used in this work. Not using any buffer salts add to the probability of finding lysozyme as monomers because of the electrostatic repulsion that inhibits dimer formation. Both surfactant and protein diffusion coefficients change in the mixed system and decrease when the surfactant-to-protein ratio is increased. The prominent features shown in Figure 2 are discussed in the following sections.

2.1. $[SOS] < 18 \text{ mM}$, $(S + L_1)$. In this region the protein is in excess and the supernatant studied by NMR contains the soluble excess protein. The complex salt Ly(OS)_8 has a low but measurable solubility in water and consequently a few surfactant molecules are also present in the supernatant.¹ The self-diffusion measurements in this region reveal the presence of lysozyme in monomeric form, with no indication of protein–surfactant association.

2.2. $18 \text{ mM} < [SOS] < 114 \text{ mM}$, $(S + L_1)$. After the point of maximum precipitation, 18 mM SOS, the surfactant is in excess. The supernatant studied contains surfactant molecules with a diffusion rate as for monomers until the protein begins to be resolubilized at a SOS concentration of 92 mM. Using NMR, a distinguishable protein peak is observed first at 114 mM SOS making it possible to determine the protein diffusion rate. The fact that it is possible to observe a protein peak shows that the precipitate has begun to be resolubilized. The somewhat slower diffusion measured compared to that of pure lysozyme indicates that surfactant molecules are bound to the protein. This clearly supports the idea that surfactant aggregation is a precondition for resolubilization. The critical concentration for association, CAC, is more accurately measured by UV spectroscopy and, as showed in Figure 1, it is possible to detect protein in the supernatant already at a total SOS concentration of 92 mM. It is important for the following discussion to note that although the diffusion of the protein–surfactant micelle is slower than that for the monomeric lysozyme molecule the diffusion rate is consistent with a micelle containing a single lysozyme molecule only, but not with larger aggregates.

2.3. $114 \text{ mM} < [SOS] < 138 \text{ mM}$, $(S + G + L_1)$, $(G + L_1)$. With a SOS concentration slightly above CAC the gel structure is a thermodynamical possibility.¹ Here it is at first in a three-phase equilibrium with remaining precipitate as a dispersion of gel-particles in a micellar supernatant. Measurements on the solution phase of this dispersion result in slower diffusion rates for surfactant molecules as well as the protein complex compared to respective monomer solutions. Hence, the surfactant binds to the protein complex. The presence of the gel structure is manifested by a broad component in the NMR spectra and by the bluish tint of the sample. The actual diffusion coefficients of the protein–surfactant micelles are however not affected by the presence of gel particles. This has been confirmed by measurements on micellar supernatants of centrifuged samples.

A decrease in diffusion coefficients is expected purely on the basis of hydrodynamic crowding effects.²² Thus, before interpreting the sudden decrease after CAC the volume fraction of aggregates in solution need to be considered. As a result of the resolubilization of the complex salt, the concentration of aggregates in the solution is increasing fast over a small interval of surfactant concentration. In fact, a plot of diffusion coefficients vs volume fraction of aggregates in solution shows a regular decrease of the measured D -values as shown in Figure 3. The decrease in D seen experimentally can thus be partly described as a crowding effect due to direct and hydrodynamic interactions. In the calculation of the effective volume fraction

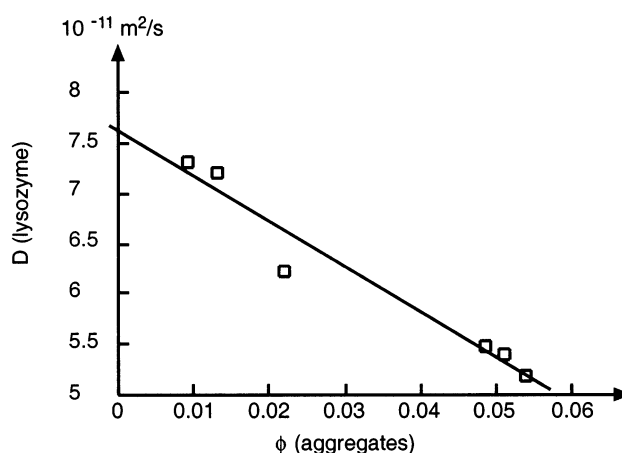


Figure 3. The measured diffusion coefficient for lysozyme vs increasing volume fraction of aggregates (lysozyme monomers or mixed micelles). The extrapolation of the decrease in lysozyme diffusion to zero volume fraction gives $D_0 \approx 7.6 \times 10^{-11} \text{ m}^2/\text{s}$.

we have considered all suspended material to be lysozyme spheres and SOS monomers are considered as solvent molecules. We have taken into account that the concentration of surfactant monomers in solution is decreasing with increasing total concentration.^{23,24}

A linear extrapolation to zero-volume fraction for the measured D -values of lysozyme, which is present in micelles only, results in the self-diffusion coefficient at $\phi = 0$, i.e., $D_0 \approx 7.5 \times 10^{-11} \text{ m}^2/\text{s}$. Using the Stokes–Einstein expression for the diffusion coefficient of a sphere we find that this corresponds to a hydrodynamic radius of 29 Å which is significantly larger than the value 23 Å determined for the hydrodynamic radius of lysozyme in water.²⁵ Thus when a SOS micelle is associated with the lysozyme molecule there is a small but significant increase in the hydrodynamic radius. This is consistent with a report on the analogue lysozyme–SDS–water system where the hydrodynamic radius of the complex was found to be 32 Å.⁴

2.4. $[SOS] > 138 \text{ mM}$ (L_1). With even higher concentrations of SOS, all material is soluble and in the single, micellar phase. The diffusion coefficients are decreasing with increasing concentration also in this region, but the calculated behavior of soft spheres indicates that this decrease can be attributed to the increased crowding. However, we cannot exclude that there is also a minor increase in SOS aggregation number of the mixed micelles. In this concentration regime pure SOS micelles start to form. These have a faster diffusion rate than the protein–surfactant complexes but due to the increasing volume fraction of aggregates the averaged diffusion coefficient of OS^- continues to decrease.

3. Modeling the Phase Equilibria. The different associative structures, the solid, the gel, and the micellar solution go through a series of mutual equilibria as the concentrations change in the experiments. NMR measurements clearly showed that the bluish solutions consisted of gel coexisting with micellar complex. With UV measurements we could conclude that the solid below CAC is in equilibrium with a premicellar surfactant solution dilute in protein. These equilibria are accessible for quantitative analysis based on the experimental results. Thus, from a model of the different structures it is possible to obtain the equilibrium chemical potential of the surfactant and in this way one can relate the phase behavior to the underlying molecular force balance affecting the associative behavior.

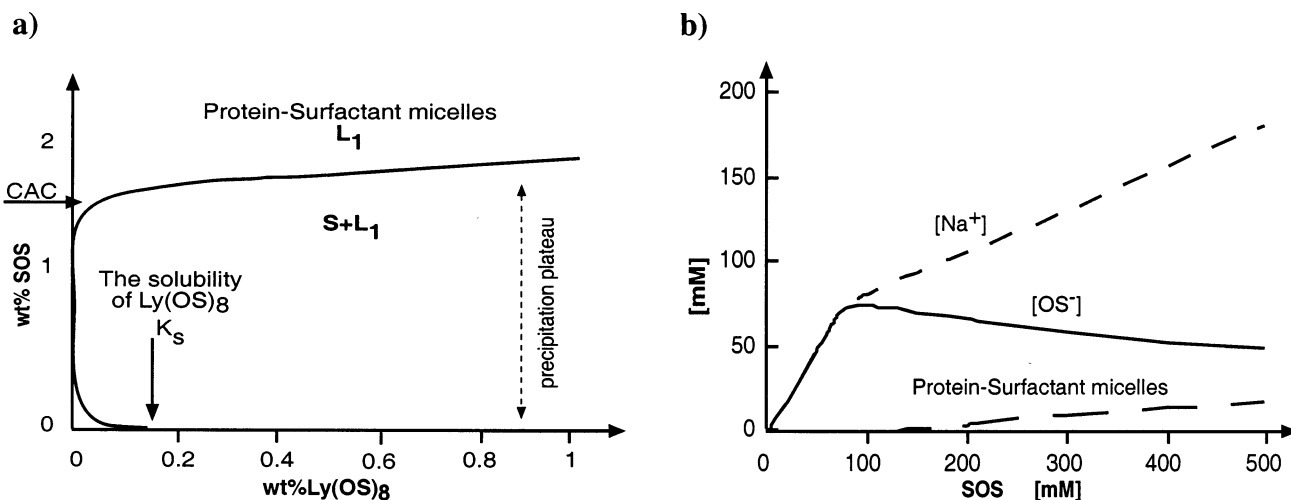
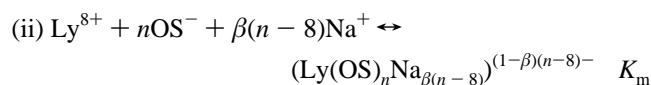
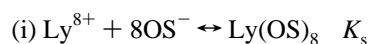


Figure 4. (a) The calculated phase border between the two-phase region $S + L_1$ and the single L_1 phase. The border is defined by the solubility product K_s , the CAC and the aggregation number of the micelles. (b) The concentration of the different ionic species on the phase border as a function of increasing SOS concentration.

3.1. Equilibrium between L_1 and $S + L_1$. Two equilibria and three mass balances describe the equilibrium that defines the phase border between the micellar solution phase and the solid complex salt.



$$C_{\text{lysozyme}}^{\text{tot}} = C_{\text{lysozyme}}^{\text{free}} + C^{\text{micelle}} \quad (3)$$

$$C_{\text{OS}^-}^{\text{tot}} = C_{\text{OS}^-}^{\text{free}} + nC^{\text{micelle}} \quad (4)$$

$$C_{\text{Na}^+}^{\text{tot}} = C_{\text{Na}^+}^{\text{free}} + \beta(n-8)C^{\text{micelle}} \quad (5)$$

The first equilibrium is characterized by a solubility product K_s of 10^{-28} M^9 determined by the solubility of the complex salt in pure water.¹ The second equilibrium is characterized by the micelle stability constant K_m that is related to the CAC and the micellar aggregation number n . The counterion binding constant, β , is set equal to 0.7.²³ From NMR and UV experiments the CAC is determined but not n . Thus, K_m is calculated for different aggregation numbers. The system of equations is solved in an iterative manner for various n and the resulting phase borders are compared to the experimental phase diagram. The calculated phase border obtained is presented in Figure 4a and represents the solution when $n = 30$ and $\log K_m = -69$. The aggregation number of 30 does not deviate significantly from that of pure SOS,²⁶ and this value is used in the following discussion. As is typical for ionic surfactants, the concentrations of free ions in solution vary in opposite directions with increased total SOS concentration as is shown in Figure 4b.²³ Using the decrease in diffusion coefficient for OS^- given by the NMR measurements of the L_1 phase and the criterion that the surfactant ion is either in mixed micelles with protein or diffusing as monomers, a consistent decrease in monomer concentration is obtained.

3.2. Equilibrium between L_1 and G . For certain equilibrium compositions, protein molecules are present in both single micelles in the L_1 phase and in a more aggregated gel state. This shows that in this particular case there is a delicate free energy balance between the two surfactant–lysozyme structures.

One criterion for equilibrium is that the chemical potential of SOS is equal in the two phases. The conditions of the solution phase are described by eqs 3–5 which yield the SOS chemical potential given the values of n and K_m . Modeling the gel phase is more problematic since we have no definite information on the molecular arrangement in the phase. However, irrespective of the structural details, surfactant and lysozyme are associated into aggregates that have a net negative charge. This charge causes an electrostatic swelling and a concentration-dependent double-layer effect. The stoichiometry of the gel complex is determined by a balance between the hydrophobic attraction and the electrostatic repulsion. The same balance is operating in the formation of the mixed micelles, and the equilibrium between the two types of structures can be qualitatively understood by quantitative modeling of the electrostatic effects.

Following our previous study with lysozyme and SDS we represent the gel phase as a lamellar system¹ within the Poisson–Boltzmann (PB) approximation.¹¹ Choosing one-dimensional cylindrical aggregates yields qualitatively the same results. For a solution of the PB equation one needs the surface charge density, the separation between the charged surfaces, and the chemical potential of the electrolyte(s) in the aqueous medium. The PB equation is solved numerically using the program package PB-cell.²⁷ On the basis of the observed composition of the gel phase we estimate 28 OS^- molecules per lysozyme in the aggregates of the gel phase. There is, in addition, monomeric OS^- in the aqueous domains between the lamellae according to eqs 3–5 and Figure 4b. The 28:1 stoichiometry correlates to a surface charge density of $1e/1.8 \text{ nm}^2$ using the same procedure as in ref 1.

The monomer concentration of OS^- in the aqueous domains is determined through the equilibrium between OS^- in the aggregate lamella and OS^- between the lamellae. Analogous to the micelle–monomer equilibrium in the isotropic solution, the equilibrium is determined by a combination of a concentration-independent hydrophobic contribution $\Delta\mu_{\text{HF}}^\theta$ and a concentration-dependent electrostatic contribution $\Delta\mu_{\text{el}}^\theta$ so that

$$k_B \ln[\text{OS}^-]_{\text{aq}} = \Delta\mu_{\text{HF}}^\theta + \Delta\mu_{\text{el}}^\theta \quad (6)$$

Using the observed composition of the isotropic solution of the three-phase triangle and the model of eqs 3–5, we determine the chemical potential of SOS in the three-phase triangle. Then

using the compositions of the gel in the second corner of the triangle, $\Delta\mu_{\text{HF}}$ is adjusted to yield the same SOS chemical potential. This requires the solution of the PB equation to determine μ_{el} . Thus we find $\Delta\mu_{\text{HF}}^{\text{G}} = -9.9k_{\text{B}}T$ and $\Delta\mu_{\text{el}}^{\text{G}} = 3.3k_{\text{B}}T$. An identical calculation using the PB approximation for a spherical system representing the mixed micelles yields $\Delta\mu_{\text{HF}}^{\text{L}_1} = -8.6k_{\text{B}}T$ and $\Delta\mu_{\text{el}}^{\text{L}_1} = 2.0k_{\text{B}}T$. Electrostatically, the spherical micelle is favored. The surface charge density is much lower in the spherical geometry in comparison with the gel aggregate, although more surfactant ions are associated with a protein molecule. Consequently, more surfactant molecules can be veiled against water with a comparably low cost in electrostatic repulsion. On the other hand, the hydrophobic interaction favors the gel aggregate. Consistent with our previous report, the structure of the gel phase is mediated by hydrophobic interactions while electrostatic swelling induces its porosity. A gel formed with SOS instead of SDS incorporates more surfactant molecules per protein (28 and 14, respectively) in the network as a result of the higher concentration of free ions in the aqueous domains. This quantitative difference between SOS and SDS can be expressed by the similar phase behavior of the two systems SDS–lysozyme–NaCl_(aq) and SOS–lysozyme–water.^{8,28}

Concluding Remarks

The dissolution of Ly(OS)₈ is by NMR diffusometry shown to be a result of SOS micellization with a corresponding CAC of 74 mM measured by UV-absorption. For the appropriate choice of aggregation number $n_{\text{mic}} = 30$ and counterion binding constant $\beta = 0.7$ the calculated phase border between the micellar L₁ phase and the two-phase S + L₁ area successfully reproduces the experimental diagram.

The equilibrium chemical potential of SOS in gel and protein–surfactant micelle is calculated by solving the PB equation. The difference in the hydrophobic contribution to the chemical potential between the two phases favors the formation of a gel. On the other hand, the possibility for the spherical micelle to host a higher number of surfactant ions per protein without increasing the surface charge density favors the mixed micelle.

The separation of the free energy in a concentration-dependent electrostatic part and a concentration-independent hydrophobic part, facilitates the comparison with analogue systems. The gel phase is in the SOS system obtained at surfactant concentrations above the system's CAC. It is a very delicate balance and it is only due to a small difference in hydrophobic free energy that the gel is formed. In the SDS system, the gel occurs below the CAC. The stability of the gel phase relative to the mixed micelles is consequently larger. For the SDS system the electrostatic part of the free energy plays a more important role due to the lower monomer concentration, which provides the background electrolyte in the ternary system. Consequently there is for SDS a much larger difference in the surfactant protein ratio in gel and in the micelles relative to what is found for SOS. That the electrostatic contribution is important in determining the stoichiometry is further supported by the observation that on adding salt the surfactant-to-protein ratio increases substantially in the gel for the SDS system.²⁸ Following this reasoning, a gel should not be observed in the system lysozyme–sodium hexyl sulfate–water in the same concentration regime. This is consistent with the reported phase diagrams by Morén et al.⁸

Jones and Manley concluded in a study of the binding of alkyl sulfates to lysozyme that for the dodecyl and decyl derivatives there was both a specific surfactant binding at low surfactant concentration and a nonspecific cooperative at higher concentrations, while for the octyl derivative only the non-specific one is observed.^{3,29} On the basis of the present study the specific binding corresponds to the precipitation of the complex salt. Since the solubility product increases with decreasing alkyl chain length and with increasing electrolyte concentration, one needs to go to higher concentrations to observe so-called specific binding for the shorter chain surfactants. Thus, the variation in the surfactant–lysozyme interactions with alkyl chain length can be understood as a quantitative effect caused by the normal variation in the hydrophobic interaction.

Acknowledgment. The authors thank Karin Bryskhe for valuable discussions and Dr. Ali Khan for initiating the NMR study. A.S. acknowledges Professor Bengt Jönsson for kindly providing and assisting with the PB-cell program. The project is financed by the Foundation of Strategic Research (SSF), Colloid & Interface Technology.

References and Notes

- (1) Stenstam, A.; Khan, A.; Wennerström, H. *Langmuir* **2001**, *17*, 7513.
- (2) Dobson, C. M. *Trends Biochem. Sci.* **1999**, *24*, 329.
- (3) Jones, M. N.; Manley, P. J. *Chem. Soc., Faraday Trans. 1* **1979**, *75*, 1736.
- (4) Valstar, A.; Brown, W.; Almgren, M. *Langmuir* **1999**, *15*, 2366.
- (5) Shirahama, K.; Tsujii, K.; Takagi, T. *J. Biochem.* **1974**, *75*, 309.
- (6) Ibel, K.; May, R. P.; Kirschner, K.; Szadkowski, H.; Mascher, E.; Lundahl, P. *Eur. J. Biochem.* **1990**, *190*, 311.
- (7) Fukushima, K.; Murata, Y.; Nishikido, N.; Sugihara, G.; Tanaka, M. *Bull. Chem. Soc. Jpn.* **1981**, *54*, 3122.
- (8) Morén, A. K.; Khan, A. *Langmuir* **1998**, *14*, 6818.
- (9) Söderman, O.; Stilbs, P. *Prog. NMR Spectrosc.* **1994**, *26*, 445.
- (10) Chen, A.; Wu, D.; Johnson, C. S., Jr. *J. Phys. Chem.* **1995**, *99*, 828.
- (11) Evans, D. F.; Wennerström, H. *The colloidal domain: where physics, chemistry and biology meet*, 2nd ed.; Wiley-VCH: New York, 1999; Chapter 3.
- (12) Tanford, C.; Wagner, M. L. *J. Am. Chem. Soc.* **1954**, *76*, 3331.
- (13) Mathis, A.; Zana, R. *Colloid Polym. Sci.* **2002**, *280*, 968.
- (14) Tanner, J. E. *J. Chem. Phys.* **1970**, *52*, 2523.
- (15) Stejskal, E. O.; Tanner, J. E. *J. Chem. Phys.* **1965**, *42*, 288.
- (16) Stilbs, P. *J. Magn. Reson.* **1998**, *135*, 236.
- (17) Stilbs, P.; Griffiths, P. C. *J. Phys. Chem.* **1996**, *100*, 8180.
- (18) Ekwall, P.; Mandell, L.; Fontell, K. *Mol. Cryst. Liq. Cryst.* **1968**, *8*, 157.
- (19) Lindman, B.; Thalberg, K. Polymer-surfactant interactions-recent developments. In *Interactions of Surfactants with Polymers and Proteins*; Goddard, E. D., Ananthapadmanabhan, K. P., Eds.; CRC Press: Boca Raton, FL, 1993.
- (20) Griffith, P. C.; Stilbs, P.; Howe, A. M.; Whitesides, T. H. *Langmuir* **1996**, *12*, 5302.
- (21) Nesmelova, I. V.; Fedotov, V. D. *Biochim. Biophys. Acta* **1998**, *1383*, 311.
- (22) Price, W. S.; Tsuchiya, F.; Arata, Y. *J. Am. Chem. Soc.* **1999**, *121*, 11503.
- (23) Sasaki, T.; Hattori, M.; Sasaki, J.; Nukina, K. *Bull. Chem. Soc. Jpn.* **1975**, *48*, 1397.
- (24) Stilbs, P.; Lindman, B. *J. Phys. Chem.* **1981**, *85*, 2587.
- (25) Tanford, C. *Physical Chemistry of Macromolecules*; John Wiley & Sons: New York, 1961.
- (26) Evans, D. F.; Wennerström, H. *The colloidal domain: where physics, chemistry and biology meet*, 2nd ed.; Wiley-VCH: New York, 1999; Chapter 4.
- (27) The computer program PB-cell was written and kindly provided by Professor Bengt Jönsson, Biophysical chemistry, Lund University, Sweden.
- (28) Morén, A. K.; Khan, A. *Langmuir* **1995**, *11*, 3636.
- (29) Dickinson, E. Proteins in solution and at interfaces. In *Interactions of Surfactants with Polymers and Proteins*; Goddard, E. D., Ananthapadmanabhan, K. P., Eds.; CRC Press: Boca Raton, FL, 1993.